Resonance Stabilization in Allyl Cation, Radical, and Anion

Alberto Gobbi and Gernot Frenking*

Contribution from the Fachbereich Chemie, Philipps-Universität Marburg, Hans-Meerwein-Strasse, D-35032 Marburg, Germany

Received February 8, 1994®

Abstract: The equilibrium structures, transition states for rotation, and selected distorted structures of the allyl cation (**1**), radical (**2**), and anion (**3**) are calculated at the HF/6-31G(d) and MP2/6-31G(d) level of theory. The electronic structure of the molecules is investigated using the topological analysis of the electron density distribution and the natural bond orbital partitioning scheme. The detailed analysis of the changes in the electronic structure upon rotation of a methylene group shows clearly that the planar forms of **1**, **2**, and **3** are strongly stabilized by π resonance. The significantly higher rotational barriers of **1** and **3** than that of **2** is explained by the charge distribution associated with the conjugation in the planar allyl ions. The statement made by Wiberg (*J. Am. Chem. Soc.* **1990**, *112*, 61) that the allyl anion has little resonance stabilization is repudiated. The rotation of a methylene group in **1** and **3** needs nearly the same energy when the CH_2 group is kept planar. The (C_{2v}) equilibrium structures **1**, **2**, and **3** need little energy to be distorted toward planar structures with alternating C–C bond lengths. The calculations prove that resonance stabilization is strong in the C_{2v} equilibrium structures *and* in the bond alternating planar forms. It is clearly shown that the C_{2v} forms of **1–3** are enforced by the σ frame; the π energy favors distorted planar structures with one long and one short C–C bond.

1. Introduction

It is well known that molecules with conjugated double bonds have a higher thermodynamic stability and are less reactive toward electrophilic agents than isomeric compounds having isolated (nonconjugated) double bonds. The standard textbook explanation for this stabilization is given in terms of resonance interactions.[1] The resonance energy of a conjugated molecule is defined as the enthalpy difference between the conjugated system and its reference state containing localized double bonds.[2]

There are some classical molecules which are frequently used to demonstrate the theory of resonance and conjugation, such as benzene and the allylic system (Figure 1). The properties of these molecules could not be understood in terms of localized bonds. The molecules are much less reactive tham comparable compounds which have localized bonds. The explanation, in terms of resonance interactions, is that the higher stability of the conjugated compounds is caused by π electronic delocalization.

Recent theoretical studies have challenged two different aspects of π resonance stabilization. One aspect concerns the role of the σ and π electrons in conjugated systems. Several groups presented theoretical arguments, which suggest that the π electronic energy in benzene favors a bond alternating geometry, with three long and three short C–C bonds, rather than a D_{6h} structure, and that the symmetric form of benzene is forced by the σ frame.[3,4] Also

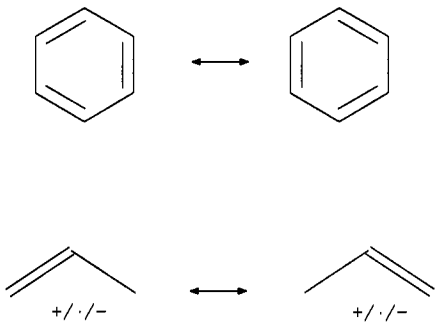

Figure 1. Resonance forms of benzene and the allyl radical.

for the allyl radical, it was concluded that the π electronic energy favors a C_s structure with one long and one short C–C bond.[3a,b,4c] It is the σ component which enforces the c_{2v} symmetry. These arguments have recently been disputed by Glendening et al.,[5] who present theoretical data which support the classical view. These authors conclude that delocalization effects act to strongly stabilize D_{6h} symmetric benzene.[5]

The role of resonance interactions has also been challenged by Wiberg[6] who published a series of papers presenting theoretical arguments against a stabilizing effect of π resonance in the allyl anion and related systems, including formaldehyde and the carboxylate anion. Wiberg analyzed the calculated data for the rotational barrier of the allyl cation and allyl anion. He concluded that "whereas the cation had significant resonance stabilization, the anion had little stabilization".[6b] He suggested that electrostatic

* Abstract published in *Advance ACS Abstracts*, September 1, 1994.

(1) (a) Vollhardt, K. P. C. *Organic Chemistry*; Freeman: New York, 1987. (b) Streitwieser, A.; Heathcock, C. H. *Introduction to Organic Chemistry*; Macmillan Publishing Company: New York, 1985. (c) March, J. *Advanced Organic Chemistry*; Wiley: New York, 1985. (d) Carey, F. A.; Sundberg, R. J. *Advanced Organic Chemistry*; Plenum Press, New York, 1990; Part A: Structure and Mechanism.

(2) Wheland, G. W. *Resonance in Organic Chemistry*; Wiley: New York, 1955.

(3) (a) Hiberty, P. C.; Ohanessian, G.; Shaik, S. S.; Flament, J. P. *Pure Appl. Chem.* **1993**, *65*, 35. (b) Shaik, S. S.; Hiberty, P. C.; Lefour, J.-M.; Ohanessian, G. *J. Am. Chem. Soc.* **1987**, *109*, 363. (c) Shaik, S. S.; Bar, R. *Nouv. J. Chim.* **1984**, *8*, 411. (d) Shaik, A. S.; Hiberty, P. C.; Ohanessian, G.; Lefour, J.-M. *Nouv. J. Chim.* **1985**, *9*, 385. (e) Hiberty, P. C.; Shaik, A. S.; Lefour, J.-M.; Ohanessian, G. *J. Org. Chem.* **1985**, *50*, 4657. (f) Shaik, A. S.; Hiberty, P. C. *J. Am. Chem. Soc.* **1985**, *107*, 3089. (g) Shaik, A. S.; Hiberty, P. C.; Ohanessian, G.; Lefour, J.-M. *J. Phys. Chem.* **1988**, *92*, 5086. (h) Ohanessian, G.; Hiberty, P. C.; Lefour, J.-M.; Flament, J.-P.; Shaik, S. S. *Inorg. Chem.* **1988**, *27*, 2219. (i) Hiberty, P. C. In *Topics in Current Chemistry*; Gutman, I., Cyrin, S. J., Eds.; Springer: New York, 1990; Vol. 153, p 27.

(4) (a) Jug, K.; Köster, A. M. *J. Am. Chem. Soc.* **1990**, *112*, 6772. (b) Stanger, A.; Vollhardt, K. P. C. *J. Org. Chem.* **1988**, *53*, 4889. (c) Heilbronner, E. *J. Chem. Educ.* **1989**, *66*, 471. (d) Epiotis, N. D. *Pure Appl. Chem.* **1983**, *55*, 229. (e) Epiotis, N. D. *Nouv. J. Chim.* **1984**, *8*, 11. For earlier studies see: (f) Longuet-Higgins, H. C.; Salem, L. *Proc. R. Soc. (London)* **1959**, *251*, 172. (g) Berry, R. S. *J. Chem. Phys.* **1961**, *35*, 29. (h) Berry, R. S. *J. Chem. Phys.* **1961**, *35*, 2253.

(5) Glendening, E. D.; Faust, R.; Streitwieser, A.; Vollhardt, K. P. C.; Weinhold, F. *J. Am. Chem. Soc.* **1993**, *115*, 10952.

(6) (a) Wiberg, K. B.; Breneman, C. M.; Laidig, K. E.; Rosenberg, R. E. *Pure Appl. Chem.* **1989**, *61*, 635. (b) Wiberg, K. B.; Breneman, C. M.; LePage T. J. *J. Am. Chem. Soc.* **1990**, *112*, 61. (c) Wiberg, K. B.; Glaser, R. *J. Am. Chem. Soc.* **1992**, *112*, 841. (d) Wiberg, K. B. *J. Am. Chem. Soc.* **1990**, *112*, 4177. (e) Wiberg, K. B.; Breneman, C. M. *J. Am. Chem. Soc.* **1992**, *114*, 831. (f) Wiberg, K. B.; Laidig, K. E. *J. Am. Chem. Soc.* **1987**, *109*, 5935. (g) Wiberg, K. B.; Rablen, P. R.; Marquez, M. *J. Am. Chem. Soc.* **1992**, *114*, 8654.

0002-7863/94/1516-9275$04.50/0 © 1994 American Chemical Society

effects are the reason for the rotational barrier in allylic anions and Y-conjugated systems.[6] However, we have recently shown that resonance stabilization in diaminomethyl cation $H_2NCHNH_2^+$, which is isoelectronic with the allyl anion, is quite strong.[7]

Because the concepts of resonance stabilization and π conjugative interactions are perhaps the most frequently used models for explaining the structures and reactivities of unsaturated compounds, we carried out a detailed theoretical analysis of the allylic system. In this paper we report the calculated structures and energies of the allyl cation ($CH_2CHCH_2^+$) radical ($CH_2CHCH_2^{\bullet}$) and anion ($CH_2CHCH_2^-$) using quantum mechanical ab initio methods. The theoretically predicted equilibrium geometries and rotational barriers have already been reported.[8] Our results are in agreement with previously reported data.[8] The focus of the present study is the electronic structure of the molecules, in particular, the effect of conjugation upon the geometries and rotational barriers. We discuss the interactions in these molecules in terms of delocalization (π resonance stabilization) and electrostatic interactions. The electronic structure of the molecules is discussed using the natural bond orbital (NBO)[9] population scheme and the topological analysis of the wave function.[10]

A major problem of theoretical studies of chemical models such as resonance and conjugation is that the subject of the investigation is not an observable quantity. This is particularly true for the concept of resonance energy, which cannot be defined in molecular orbital theory without arbitrary assumptions. The results of such studies cannot be labeled as right or wrong, but only if they are useful for the understanding of chemical phenomena or not. We want to demonstrate in this study that resonance stabilization in the allyl system is a very useful model, which explains the stability of these molecules in a plausible way.

2. Theoretical Details

The geometry optimizations and energy calculations have been carried out using the program package Gaussian 92.[11] We optimized the geometries and calculated the vibrational frequencies at the Hartree–Fock (HF) and MP2 (Møller–Plesset perturbation theory terminated at second order)[12] level of theory using a 6-31G(d) basis set.[13] The spin-restricted HF (RHF) method was used for the closed-shell compounds, while spin-unrestricted (UHF) wave functions are employed for the allyl radical. The zero-point vibrational energies (ZPE) calculated at MP2/6-31G(d) are scaled by 0.92, the ZPE data calculated at HF/6-31G(d) are scaled by 0.89.[14] Unless otherwise noted, results are discussed at MP2/6-31G(d).

For the calculation of the electron density distribution $\rho(\mathbf{r})$, the gradient vector field $\nabla\rho(\mathbf{r})$, and its associated Laplacian $\nabla^2\rho(\mathbf{r})$, the programs PROAIM, SADDLE, GRID, CUBE, and GRDVEC were used.[15] The covalent bond orders P_{CC} have been calculated using the program Bonder.[16] The NBO analysis[9] was carried out with the subroutine available in Gaussian 92.[11]

3. Allyl Cation

Table 1 shows the calculated results for the allyl cation (**1**). Figure 2 shows the optimized structures. The theoretically predicted geometry of **1** is in good agreement with previous calculations.[8a-c] The allyl cation has a planar geometry with C_{2v} symmetry (Figure 2). The C–C bond length is predicted as 1.373 Å at HF/6-31G(d) and 1.382 Å at MP2/6-31G(d). The covalent bond order for the C–C bonds is $P_{CC} = 1.439$, which agrees with the usual interpretation that the C–C bonds in **1** have a σ type single bond and one half of a π bond. The charge distribution given by the NBO and the topological analysis indicate that most of the positive charge in **1** is localized at the terminal CH_2 groups. But the two methods differ strongly concerning the charge concentration at the central CH group (Table 1). The topological analysis finds a positive charge of +0.227, while the NBO analysis gives a negative charge of –0.173 for the CH group. The NBO partitioning scheme predicts a strongly negative charge at C^1 (–0.463), while the topological analysis suggests a positive charge of +0.055 at C^1 (Table 1). The different charge distribution is due to the different criteria of the NBO method and the topological analysis used to assign the electronic charge in the C–C bonding regions to the carbon atoms.

The results of the topological analysis of the electron density distribution are shown in Table 2. Figure 3a shows the contour line diagram of the Laplacian distribution of **1** in the plane of the C–C π bond, i.e. the plane perpendicular to the molecular plane. The shape of the Laplacian distribution shows clearly that the C^1–C^3 π bond is polarized toward the central C^1 atom. The area of charge concentration ($\nabla^2\rho(\mathbf{r}) < 0$, solid lines) has a "hole" in the π direction at the terminal C^3 atom. The location of the bond critical point is slightly shifted toward C^1 ($r_b = 0.479$, Table 2). The ellipticity at the bond critical point ($\epsilon_b = 0.152$) indicates the partial π character of the C–C bonds. The energy density at the bond critical point $H_b = -2.438$ demonstrates that the C–C bond is covalent. It has been suggested that covalent bonds are characterized by strongly negative energy densities at the bond critical point H_b, whereas closed-shell interactions in ions or van der Waals complexes have values of $H_b \geq 0$.[17]

We optimized the geometry of the transition state for rotation of one CH_2 group of the allyl cation **1a** at the HF/6-31G(d) level of theory. At correlated levels **1a** is not a stationary point on the potential energy hypersurface. At the MP2/6-31G(d) level, **1a** collapses toward a hydrogen-bridged energy-minimum structure.[8c]

Structure **1a** is 34.0 kcal/mol [HF/6-31G(d)] higher in energy than **1**. At the MP2/6-31G(d) level, using geometries optimized at HF/6-31G(d), the rotational barrier is 37.8 kcal/mol (Table 1). The transition state **1a** has one short (1.318 Å) and one long (1.445 Å) C–C bond. The short C–C bond has a bond order $P_{C^1C^2} = 1.784$ and the long C–C bond has $P_{C^1C^3} = 1.153$. The positive charge at the rotated CH_2 group has increased by 0.33 e using the NBO model and by 0.17 e using the topological analysis. The shape of the Laplacian distribution in the $C^1C^2C^3$ plane (Figure 3b) shows that the hole in the π direction at C^3 has increased upon rotation. This is because there is practically no π charge at C^3. The ellipticity of the C^1–C^3 bond at the bond critical point is only $\epsilon_b = 0.008$, while the C^1–C^2 bond has $\epsilon_b = 0.404$. All calculated data indicate that the rotation of the C^1–C^3 bond in the allyl cation to the perpendicular form yields a C^1–C^2 double bond and a C^1–C^3 single bond.

(7) Gobbi, A.; Frenking, G. *J. Am. Chem. Soc.* **1993**, *115*, 2362.
(8) (a) Dorigo, A. E.; Houk, K. N. *J. Am. Chem. Soc.* **1989**, *111*, 6942. (b) Krishnan, R.; Whiteside, R. A.; Pople, J. A.; Schleyer, P. v. R. *J. Am. Chem. Soc.* **1981**, *103*, 5649. (c) Foresman, J. B.; Wong, M. W.; Wiberg, K. B.; Frisch, M. J. *J. Am. Chem. Soc.* **1993**, *115*, 2220. (d) González-Luque, R.; Nebot-Gil, I.; Merchán, M.; Tomás, F. *Theor. Chim. Acta* **1968**, *69*, 101. (e) Schleyer, P. v. R. *J. Am. Chem. Soc.* **1985**, *107*, 4793. (f) Feller, D.; Davidson, E. R.; Borden, W. T. *J. Am. Chem. Soc.* **1984**, *106*, 2513.
(9) Reed, A. E.; Curtiss, L. A.; Weinhold, F. *Chem. Rev.* **1988**, *88*, 899.
(10) Bader, R. F. W. *Atoms in Molecules: A Quantum Theory*; Oxford University Press: Oxford, 1990.
(11) Frisch, M. J.; Trucks, G. W.; Head-Gordon, M.; Gill, P. M. W.; Wong, M. W.; Foresman, J. B.; Johnson, B. G.; Schlegel, H. B.; Robb, M. A.; Replogle, E. S.; Gomperts, R.; Andres, J. L.; Raghavachari, K.; Binkley, J. S.; Gonzalez, C.; Martin, R. L.; Fox, D. J.; Defrees, D. J.; Baker, J.; Stewart, J. J. P.; Pople, J. A. *Gaussian 92*, Revision C; Gaussian, Inc.: Pittsburgh, PA, 1992.
(12) (a) Møller, C.; Plesset, M. S. *Phys. Rev.* **1934**, *46*, 618. (b) Binkley, J. S.; Pople, J. A. *Int. J. Quantum Chem.* **1975**, *9S*, 229.
(13) (a) Hehre, W. J.; Ditchfield, R.; Pople, J. A. *J. Chem. Phys.* **1972**, *56*, 2257. (b) Hariharan, P. C.; Pople, J. A. *Theor. Chim. Acta* **1973**, *28*, 213. (c) Gordon, M. S. *Chem. Phys. Lett.* **1980**, *76*, 163.
(14) Hout, R. F.; Levi, B. A.; Hehre, W. J. *J. Comput. Chem.* **1982**, *3*, 234.
(15) Biegler-König, F. W.; Bader, R. F. W.; Ting-Hua, T. *J. Comput. Chem.* **1982**, *3*, 317.
(16) (a) Cioslowski, J. BONDER; Florida State University, 1991. (b) Cioslowski, J.; Nixon, S. T. *J. Am. Chem. Soc.* **1991**, *113*, 4142.
(17) Cremer, D.; Kraka, E. *Angew. Chem.* **1984**, *96*, 612; *Angew. Chem., Int. Ed. Engl.* **1984**, *23*, 627.

Table 1. Calculated Results for the Allyl Cations **1–1c**[a]

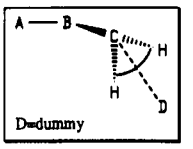

	1	**1a**	**1b**	**1c**
sym	C_{2v}	C_s	C_s	C_s
E_{tot}	−116.55762 (−116.19321)	(−116.13899)	(−116.18676)	(−116.13220)
E_{rel}	0.0 (0.0) *0.0*	(34.0) *37.8*	(4.0) *4.4*	(38.3) *38.7*
i	0 (0)	(1)		
ZPE	40.4 (41.0)	(39.2)		
C^1–C^2	1.382 (1.373)	(1.318)	(1.318)	(1.373)
C^1–C^3	1.382 (1.373)	(1.445)	(1.445)	(1.373)
C^2–C^1–C^3	117.6 (118.1)	(127.9)	(118.0)	(122.2)
C^1–C^3–D	180.0 (180.0)	(176.0)	(180.0)	(175.5)
$P_{c^1c^2}$	1.439	1.784	1.498	1.747
$P_{c^1c^3}$	1.439	1.153	1.381	1.227

	1		**1a**		**1b**		**1c**	
	$q(\rho(r))$	q(NBO)	$q(\rho(r))$	q(NBO)	$q(\rho(r))$	q(NBO)	$q(\rho(r))$	q(NBO)
C^1	0.055	−0.463	−0.130	−0.494	0.051	−0.454	−0.083	−0.532
C^2	0.015	0.088	0.067	−0.251	0.005	0.007	0.035	−0.224
C^3	0.015	0.088	0.075	0.429	0.022	0.163	0.029	0.407
H^4	0.172	0.290	0.210	0.322	0.172	0.290	0.234	0.343
H^5	0.195	0.258	0.159	0.268	0.186	0.261	0.166	0.267
H^6	0.177	0.240	0.134	0.243	0.166	0.240	0.148	0.247
H^7	0.177	0.240	0.243	0.241	0.189	0.239	0.235	0.246
H^8	0.195	0.258	0.243	0.241	0.206	0.254	0.235	0.246
C^1H^4	0.227	−0.173	0.080	−0.172	0.223	−0.164	0.151	−0.189
C^2H_2	0.387	0.586	0.360	0.260	0.357	0.508	0.349	0.290
C^3H_2	0.387	0.586	0.561	0.911	0.417	0.656	0.499	0.899

[a] Calculated total energies, E_{tot} (hartrees); relative energies, E_{rel} (kcal/mol); number of imaginary frequencies, i; zero-point energies, ZPE (kcal/mol) calculated bond lengths, C–C (Å); angles C–C–C (deg); folding angle of the C^3H_2 group C^1–C^3–D (deg); covalent bond orders P_{CC}; partial charges from the NBO analysis q(NBO) and from the topological analysis $q(\rho(r))$. Energies and geometries are given at MP2/6-31G(d). Values at HF/6-31G(d) are shown in parentheses; energies at MP2/6-31G(d)//HF/6-31G(d) are given in italics. The bond orders P_{CC} and the topological charges $q(\rho(r))$ are given at MP2/6-31G(d)//HF/6-31G(d). The charges derived from the NBO analysis are given at HF/6-31G(d)//HF/6-31G(d).

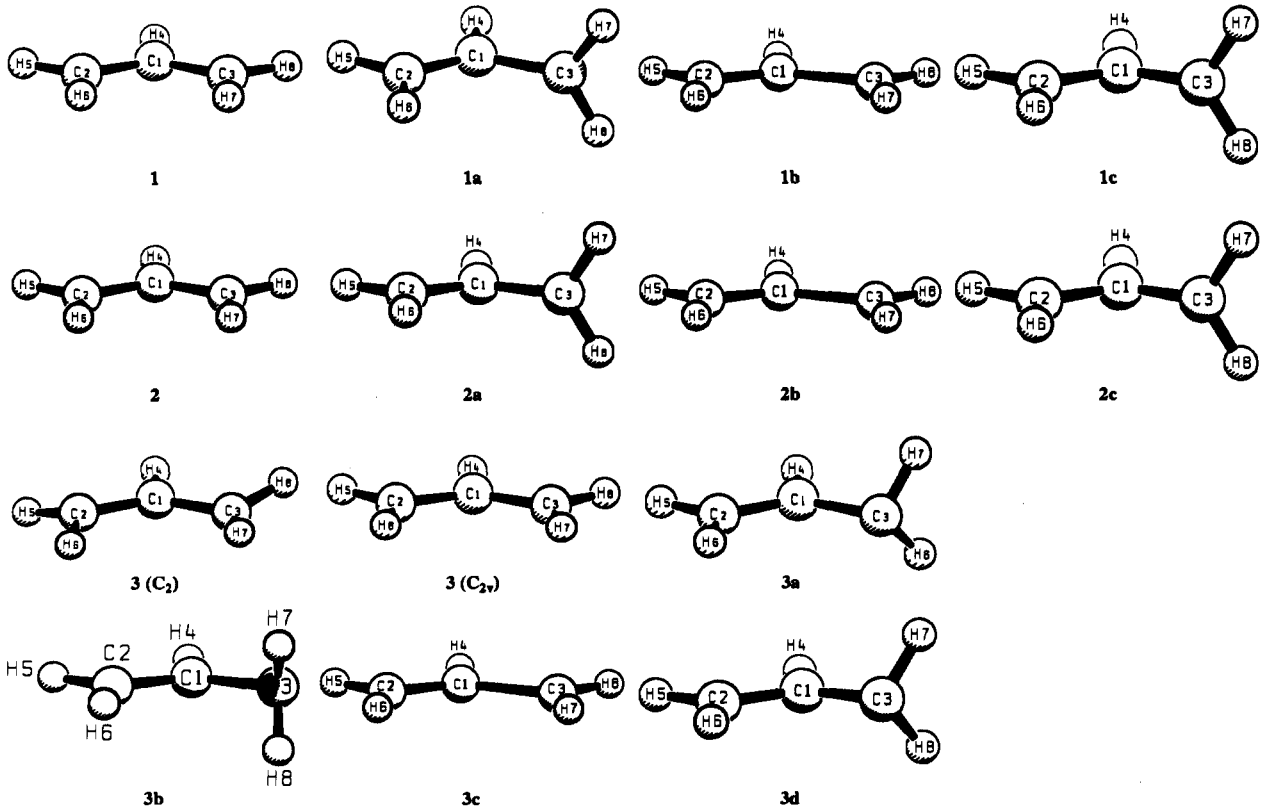

Figure 2. Optimized structures of the allyl cation (**1**), radical (**2**), and anion (**3**).

An interesting feature of the rotated C^1–C^3 bond is the polarization of the σ charge in **1a**. The shape of the Laplacian distribution (Figure 3b) shows that the C^1–C^3 σ bond of **1a** is polarized toward the terminal C^3H_2 group. Also the location of

Table 2. Results of the Topological Analysis for the Allyl Cation (**1**), Radical (**2**), and Anion (**3**) and Related Structures Calculated at MP2/6-31G(d)//HF/6-31G(d)[a]

	1				2				3			
	ρ_b	H_b	r_b	ϵ_b	ρ_b	H_b	r_b	ϵ_b	ρ_b	H_b	r_b	ϵ_b
C^1–C^2	2.223	−2.438	0.479	0.152	2.102	−2.175	0.502	0.253	2.076	−2.177	0.520	0.400
C^1–H^4	1.944	−2.143	0.670	0.008	1.905	−2.008	0.646	0.007	1.803	−1.823	0.624	0.006
C^2–H^5	1.971	−2.216	0.679	0.022	1.902	−2.012	0.646	0.024	1.783	−1.810	0.619	0.106
C^2–H^6	1.963	−2.187	0.675	0.022	1.893	−1.994	0.646	0.022	1.778	−1.795	0.621	0.096
	1a				**2a**				**3a**			
	ρ_b	H_b	r_b	ϵ_b	ρ_b	H_b	r_b	ϵ_b	ρ_b	H_b	r_b	ϵ_b
C^1–C^2	2.283	−2.783	0.540	0.404	2.328	−2.695	0.508	0.597	2.336	−2.792	0.486	0.397
C^1–C^3	1.932	−2.080	0.433	0.008	1.814	−1.636	0.503	0.047	1.643	−1.514	0.555	0.138
C^1–H^4	1.761	−1.836	0.664	0.015	1.887	−1.979	0.647	0.001	1.751	−1.704	0.626	0.006
C^2–H^5	1.934	−2.119	0.666	0.005	1.904	−2.015	0.646	0.000	1.813	−1.842	0.626	0.033
C^2–H^6	1.926	−2.084	0.662	0.002	1.904	−2.015	0.647	0.000	1.851	−1.914	0.637	0.035
C^3–H^7	1.978	−2.279	0.691	0.043	1.879	−1.974	0.648	0.038	1.637	−1.550	0.611	0.096
	1b				**2b**				**3c**			
	ρ_b	H_b	r_b	ϵ_b	ρ_b	H_b	r_b	ϵ_b	ρ_b	H_b	r_b	ϵ_b
C^1–C^2	2.465	−3.008	0.481	0.170	2.360	−2.765	0.506	0.346	2.293	−2.668	0.520	0.409
C^1–C^3	1.941	−1.872	0.476	0.138	1.788	−1.587	0.499	0.173	1.627	−1.352	0.519	0.392
C^1–H^4	1.946	−2.149	0.670	0.008	1.907	−2.014	0.646	0.007	1.815	−1.837	0.626	0.008
C^2–H^5	1.964	−2.193	0.676	0.020	1.897	−2.000	0.645	0.016	1.786	−1.808	0.620	0.088
C^2–H^6	1.956	−2.164	0.672	0.020	1.891	−1.987	0.645	0.014	1.789	−1.810	0.623	0.080
C^3–H^7	1.969	−2.211	0.678	0.024	1.895	−2.003	0.647	0.030	1.781	−1.808	0.621	0.115
C^3–H^8	1.656	−2.240	0.681	0.024	1.904	−2.021	0.647	0.032	1.785	−1.819	0.620	0.124
	1c				**2c**				**3d**			
	ρ_b	H_b	r_b	ϵ_b	ρ_b	H_b	r_b	ϵ_b	ρ_b	H_b	r_b	ϵ_b
C^1–C^2	2.026	−2.172	0.467	0.402	2.066	−2.114	0.501	0.366	2.123	−2.240	0.486	0.397
C^1–C^3	2.213	−2.792	0.422	0.004	2.124	−2.229	0.500	0.023	2.090	−2.577	0.578	0.188
C^1–H^4	1.712	−1.764	0.666	0.007	1.854	−1.916	0.643	0.020	1.701	−1.605	0.625	0.001
C^2–H^5	1.943	−2.142	0.668	0.009	1.896	−2.004	0.645	0.022	1.815	−1.848	0.627	0.039
C^2–H^6	1.933	−2.109	0.665	0.007	1.894	−1.999	0.646	0.021	1.848	−1.910	0.636	0.039
C^3–H^7	1.965	−2.240	0.689	0.041	1.869	−1.950	0.646	0.037	1.632	−1.547	0.611	0.102

[a] Charge density at the bond critical point, ρ_b (e/Å^3); energy density at the bond critical point, H_b (hartree/Å^3); location of the bond critical point r_b for the bond A–B given by A – r_b/A – B; ellipticity at the bond critical point, ϵ_b.

the bond critical point r_b of the C^1–C^3 bond is shifted toward C^1 (r_b = 0.433, Table 2). This is because the electron-deficient C^3H^2 group has become more electronegative upon rotation. The bond critical point of the C^1–C^2 bond has migrated in the opposite direction toward the terminal C^2 atom (r_b = 0.540). The opposite polarization and the equilibrium of the σ and π charges in allyl ions has been discussed in detail by Slee and MacDougall.[18]

In order to study the changes in the electronic structure upon rotation of the CH_2 group in greater detail, we calculated two different structures **1b** and **1c**. Structure **1b** has a planar geometry with one long and one short C–C bond length taken from the optimized transition state **1a**. Structure **1c** has the same C–C bond lengths as the energy minimum form **1**, but one CH_2 group is rotated. The geometries of **1b** and **1c** are optimized at the HF/6-31G(d) level with the constraints of the C–C bond distances being frozen.

Table 1 shows that **1b** is only 4.4 kcal/mol [MP2/6-31G(d)//HF/6-31G(d)] higher in energy than **1**. This means that the deformation of the C_{2v} form **1** toward a structure with one long and one short C–C bond needs very little energy compared with the rotational barrier. The same holds true for the calculated energy of **1c**. The rotated structure **1c**, with the same C–C distances as in the allyl cation **1**, is only 0.9 kcal/mol [MP2/6-31G(d)//HF/6-31G(d)] higher in energy than the transition state **1a** (Table 1).

The analysis of the electronic structures of **1b** and **1c** reveals interesting details (Table 2). The C–C bond orders P_{CC} for the C^1–C^2 and C^1–C^3 bonds in **1b** are not very different ($P_{C^1C^2}$ = 1.498, $P_{C^1C^3}$ = 1.381) from the values in **1** (P_{CC} = 1.439). This means that the π bonding character of the elongated C^1–C^3 bond is not reduced as much as one might anticipate. Also the charges at the terminal CH_2 groups in **1b** are not very different from the calculated charges of **1** (Table 1). Similar conclusions can be drawn from the results calculated for **1c**. The covalent bond orders P_{CC} for the C–C bonds of **1c** ($P_{C^1C^2}$ = 1.747, $P_{C^1C^3}$ = 1.227) are similar to the P_{CC} values calculated for **1a** ($P_{C^1C^2}$ = 1.784, $P_{C^1C^3}$ = 1.153). Also the ellipticities of the C–C bonds of **1b** and **1c** are comparable to the corresponding values of **1** and **1a**, respectively. The Laplacian distribution in the π plane of the C^1–C^2 and C^1–C^3 bonds of **1b** are very similar (Figure 3, parts c and d).

The analysis of the calculated structures **1**–**1c** shows clearly that the deformation of the C_{2v} form **1** toward a planar structure with alternating C–C bond lengths **1b** needs rather little energy and that there is strong resonance stabilization in **1** *and* **1b**, while the rotational barrier is high.

4. Allyl Radical

Table 3 shows the optimized geometries and structural data for the energy minimum structure of the allyl radical (**2**) and the distorted allyl radical **2a**, where one methylene group is rotated by 90°. The energy minimum structure **2** has C_{2v} geometry with calculated C–C bond lengths of 1.391 Å [HF/6-31G(d)] and 1.377 Å [MP2/6-31G(d)]. The NBO method suggests that the CH_2 groups carry a small positive partial charge (+0.040). The topological analysis finds a small negative charge of −0.013 for the methylene groups of **2** (Table 3). The covalent bond order for the C–C bonds of **2** is slightly larger (P_{CC} = 1.448) than for the allyl cation **1** (P_{CC} = 1.439). The energy density at the bond

(18) Slee, T. S.; MacDougall, P. J. *Can. J. Chem.* **1988**, *66*, 2961.

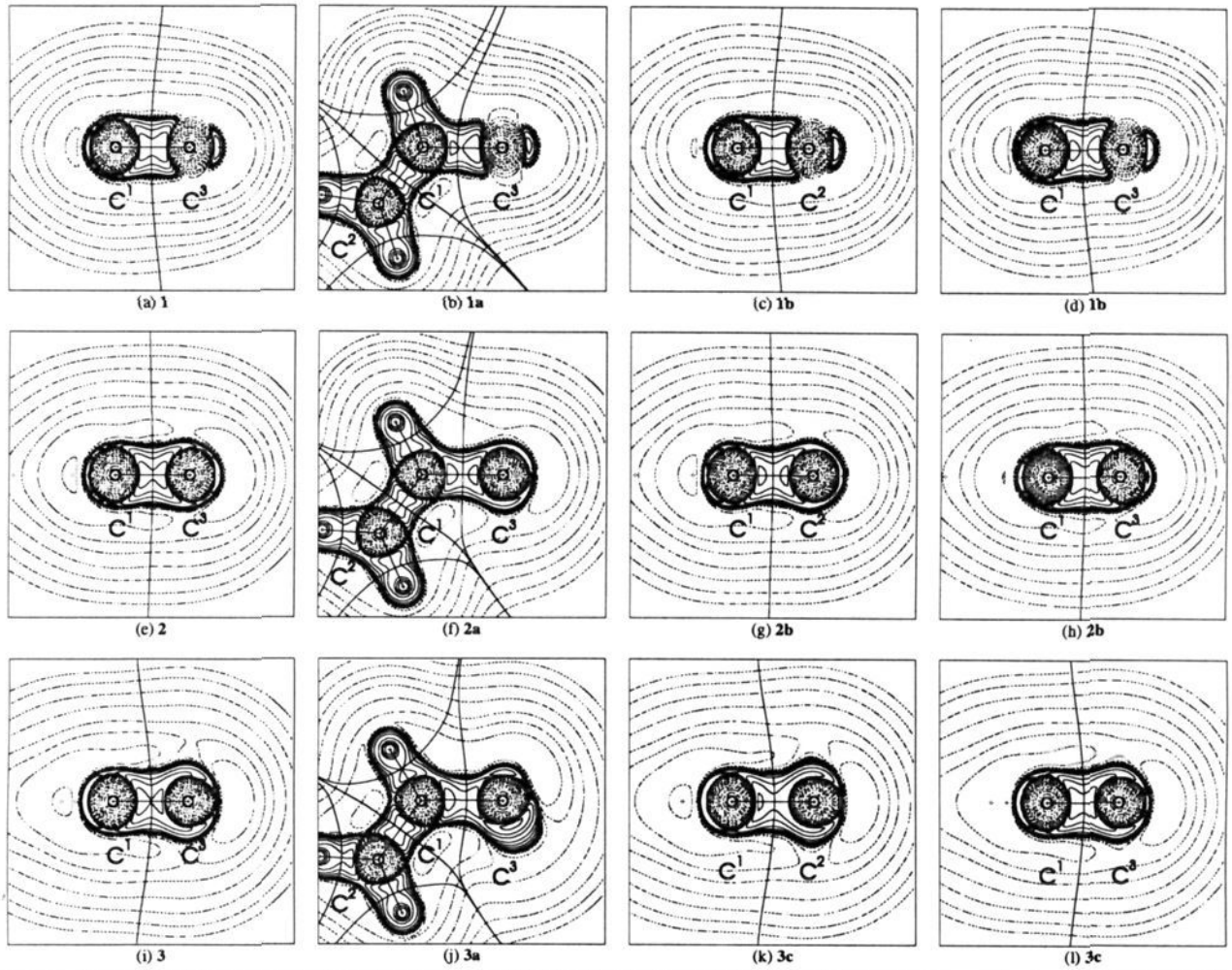

Figure 3. Contour line diagrams of the Laplacian distribution $\nabla^2\rho(\mathbf{r})$ at MP2/6-31G(d)//HF/6-31G(d): (a) structure **1** (π plane of the C^1–C^3 bond); (b) structure **1a** (C^2–C^1–C^3 plane); (c) structure **1b** (π plane of the C^1–C^2 bond); (d) structure **1b** (π plane of the C^1–C^3 bond); (e) structure **2** (π plane of the C^1–C^3 bond); (f) structure **2a** (C^2–C^1–C^3 plane); (g) structure **2b** (π plane of the C^1–C^2 bond); (h) structure **2b** (π plane of the C^1–C^3 bond); (i) structure **3** (π plane of the C^1–C^3 bond); (j) structure **3a** (C^2–C^1–C^3 plane); (k) structure **3c** (π plane of the C^1–C^2 bond); (l) structure **3c** (π plane of the C^1–C^3 bond). Dashed lines indicate charge depletion ($\nabla^2\rho(\mathbf{r}) > 0$); solid lines indicate charge concentration ($\nabla^2\rho(\mathbf{r}) < 0$). The solid lines connecting the atomic nuclei are the bond paths; the solid lines separating the atomic nuclei indicate the zero-flux surfaces in the plane. The crossing points of the bond paths and zero-flux surfaces are the bond critical points $\mathbf{r}_b$.

critical point for the CC bonds of **1** ($H_b = -2.175$) is less negative than in **2** ($H_b = -2.438$).

The contour line diagram of **2** in the plane of the C–C π bond (Figure 3e) shows an obvious difference from the C–C bond of **1** (Figure 3a). The hole in the electron density of the valence sphere around C^3 has disappeared. This is because the unpaired electron in **2** occupies a π MO which is localized at the terminal carbon atoms (see Figure 4). The position of the bond critical point $\mathbf{r}_b$ shows that the C–C bonds in **2** are nearly nonpolar ($\mathbf{r}_b = 0.502$, Table 2). The π contribution to the C–C bonds in **2** is clearly higher than in **1**, which is revealed by the calculated ellipticity for the C–C bonds of **2** ($\epsilon_b = 0.253$).

The energy barrier for rotation of a CH_2 group of the allyl radical is predicted as 18.6 kcal/mol at HF/6-31G(d). Structure **2a** is a transition state at HF/6-31G(d). The energy difference between **2** and **2a** reduces to 12.1 kcal/mol at MP2/6-31G(d). The rotated form **2a** is a spurious minimum on the potential energy hypersurface at MP2/6-31G(d). The transition state for rotation of a methylene group at MP2/6-31G(d) has a torsion angle of 61.2°, and it is 12.7 kcal/mol higher in energy than **2**. A similar value for the rotational barrier is predicted at MP2/6-31G(d) using the HF/6-31G(d) optimized geometries (12.6 kcal/mol). This is gratifying, because it shows that HF/6-31G(d)-optimized geometries may be used in conjunction with energies calculated at MP2/6-31G(d). The calculated rotational barrier for the allyl radical (12.7 kcal/mol) is in reasonable agreement with the previously reported value of 14.1 kcal/mol, which was calculated at the MCSCF/DZP level of theory.[8f]

The optimized geometry of **2a** has one short C–C bond [1.327 Å at HF/6-31G(d), 1.305 Å at MP2/6-31G(d)] and one long C–C bond [1.479 Å at HF/6-31G(d), 1.475 Å at MP2/6-31G(d)]. There are larger changes in the covalent bond orders P_{CC} for the allyl radical upon rotation than for the allyl cation. The P_{CC} values of **2a** are 2.113 and 1.074 for the short and long C–C bond, respectively. The corresponding values for the C–C bond orders in **1a** are 1.784 and 1.153 (Table 1). The NBO method and the topological analysis suggest that the rotated CH_2 group carriers a slightly higher positive charge in **2a** (by 0.017 e) than in **2**.

The shape of the Laplacian distribution of **2a** shown in Figure 3f indicates a shift of electronic charge from the π bonding region of the C^1–C^3 bond toward the terminal carbon atom C^3. The ellipticity of the C^1–C^3 bond is greatly reduced ($\epsilon_b = 0.047$), but the position of the bond critical point indicates that the overall polarity of the C^1–C^3 bond ($\mathbf{r}_b = 0.503$) is nearly the same as in **2**. This is because the σ and π contributions to the C–C bond migrate in opposite direction upon rotation.[18] All calculated data of the electronic structure of **2** and **2a** suggest that the only

Table 3. Calculated Results for the Allyl Radicals 2–2c (For Details see Table 1)

	2	2a	2b	2c
sym	C_{2v}	C_s	C_s	C_s
E_{tot}	−116.82429(−116.46810)	−116.80506(−116.43851)	(−116.46136)	(−116.42684)
E_{rel}	0.0 (0.0) *0.0*	12.1 (18.6) *12.6*	(4.2) *3.6*	(25.9) *14.6*
i	0 (0)	0 (1)		
ZPE	39.2 (38.8)	40.8 (38.0)		
C^1–C^2	1.377 (1.391)	1.305 (1.327)	(1.327)	(1.391)
C^1–C^3	1.377 (1.391)	1.475 (1.479)	(1.479)	(1.391)
C^2–C^1–C^3	124.4 (124.5)	125.0 (124.8)	(124.3)	(125.5)
C^1–C^3–D	180.0 (180.0)	165.3 (167.9)	(180.0)	(168.6)
$P_{C^1C^2}$	1.448	2.113	1.752	1.763
$P_{C^1C^3}$	1.448	1.074	1.175	1.098

	2		2a		2b		2c	
	$q(\rho(r))$	q(NBO)	$q(\rho(r))$	q(NBO)	$q(\rho(r))$	q(NBO)	$q(\rho(r))$	q(NBO)
C^1	−0.022	−0.294	−0.061	−0.277	−0.030	−0.286	−0.034	−0.284
C^2	−0.128	−0.344	−0.105	−0.400	−0.104	−0.368	−0.117	−0.407
C^3	−0.128	−0.344	−0.144	−0.305	−0.146	−0.327	−0.130	−0.307
H^4	0.048	0.214	0.055	0.212	0.049	0.214	0.046	0.215
H^5	0.059	0.195	0.054	0.206	0.054	0.200	0.052	0.208
H^6	0.056	0.189	0.057	0.204	0.051	0.194	0.055	0.205
H^7	0.056	0.189	0.074	0.181	0.064	0.184	0.065	0.185
H^8	0.059	0.195	0.074	0.181	0.065	0.189	0.065	0.185
C^1H^4	0.026	−0.080	−0.006	−0.065	0.019	−0.072	0.012	−0.069
C^2H_2	−0.013	0.040	0.006	0.010	0.001	0.026	−0.010	0.006
C^3H_2	−0.013	0.040	0.004	0.057	−0.017	0.046	0.000	0.063

significant change upon rotation of the CH_2 group is the partitioning of the π bond contribution toward a C^1–C^2 double bond (ϵ_b = 0.597, $P_{C^1C^2}$ = 2.113) and a C^1–C^3 single bond (ϵ_b = 0.047, $P_{C^1C^2}$ = 1.074).

We calculated the planar species **2b**, which has C–C bond lengths taken from **2a**, and the twisted structure, **2c**, having the same bond lengths as the allyl radical **2** (Table 2). The rest of the molecules are optimized at HF/6-31G(d). The energy difference between **2b** and **2** is only 3.6 kcal/mol [MP2/6-31G(d)//HF/6-31G(d)], which is very similar to the energy difference between **1** and **1b** (4.4 kcal/mol, Table 1). The calculated bond order for the shortened C^1–C^2 bond in **2b** ($P_{C^1C^2}$ = 1.752) is significantly increased relative to **2** (P_{CC} = 1.448). The bond order for the stretched C^1–C^3 bond is reduced by nearly the same amount ($P_{C^1C^3}$ = 1.175). Still, the C^1–C^3 bond has a significant π contribution as revealed by the calculated ellipticity ϵ_b = 0.173 (Table 2). The charge distribution in **2b** is very similar to that in **2** (Table 3).

The twisted structure **2c** is only 2.0 kcal/mol higher in energy than **2a** (Table 3). The C^1–C^3 bond of the rotated methylene group has a bond order $P_{C^1C^3}$ = 1.098, which is nearly the same value as that calculated for the C^1–C^3 single bond in **2a** ($P_{C^1C^3}$ = 1.074). There is very little π contribution to the C^1–C^3 bond in **2c** as revealed by the ellipticity ϵ_b = 0.023. The ellipticity of the C^1–C^2 bond is very high (ϵ_b = 0.366). The charge distribution of **2c** differs very little from **2a**.

The calculated data for **2**–**2c** shows that the allyl radical also needs much less energy for the distortion from the C_{2v} equilibrium **2** toward **2b** than for rotation around the C–C bond, and that there is significant resonance stabilization in the bond alternating form **2b**, as for the allyl cation. However, the rotational barrier is much lower for **2** than for **1**.

5. Allyl Anion

The calculated data for the allyl anion **3** and other $C_3H_5^-$ structures are shown in Table 4. At the HF/6-31G(d) level of theory, **3** has C_{2v} symmetry with C–C bond lengths of 1.382 Å. The planar C_{2v} form of **3** is not a minimum on the potential energy hypersurface at MP2/6-31G(d). There are two imaginary modes associated with the out-of-plane motion of the CH_2 groups. The energy-minimum structure of **3** at MP2/6-31G(d) has C_2 symmetry and pyramidal methylene groups. However, the pyramidal form is, at MP2/6-31G(d), only 0.2 kcal/mol lower in energy than the planar structure. The planar form becomes more stable than the pyramidal energy-minimum structure at MP2/6-31G(d) when corrections are made for zero-point vibrational energies (Table 4).

Both methods, NBO and topological analysis, show that the negative charge is located mainly at the terminal CH_2 groups. The C–C covalent bond order of the allyl anion is calculated to be significantly higher (P_{CC} = 1.652) than for the cation (P_{CC} = 1.439) and the radical (P_{CC} = 1.448). Also the ellipticity of the C–C bonds of **3** (Table 2) is much higher (ϵ_b = 0.400) than for **1** (ϵ_b = 0.152 and **2** (ϵ_b = 0.253) reflecting the changing population of the π MO. The contour line diagram of **3** in the π plane of the C–C bond, shown in Figure 3i, demonstrates clearly the differences compared with the C–C bonds of **1** (Figure 3a) and **2** (Figure 3e). The π bond is clearly polarized toward the terminal carbon atom. However, the bond critical point r_b is shifted away from the central carbon atom toward the terminal carbon atom (r_b = 0.520), which indicates that the central carbon atom has a higher electronegativity than the terminal carbon atoms. The opposite polarization of the σ and π charge of the C–C bonds is indicated for **1** (Figure 3a). The energy density at the bond critical point of the C–C bonds in **3** (H_b = −2.177) is nearly the same as in **2** (H_b = −2.175).

The transition state for rotation of a methylene group of **3** has strongly pyramidal CH_2 groups. There are two transition states **3a** and **3b** for the inward and outward rotation of the electron lone pair which is formed during the rotation (Figure 2). The inward rotation is energetically favored. Transition state **3a** is 23.1 kcal/mol [MP2/6-31G(d)//HF/6-31G(d)] higher in energy than **3**. The outward rotation toward **3b** has a barrier of 25.4 kcal/mol [MP2/6-31G(d)//HF/6-31G(d)]. The Laplacian distribution for the transition state **3a**, shown in Figure 3j, visualizes the formation of the electron lone-pair at the rotated methylene group. The partial negative charge at the rotated CH_2 group has increased in **3a** by 0.274 e (NBO) or 0.162 e (topological analysis) relative to **3** (Table 4). The covalent bond order of the C^1–C^3 bond of **3a** is reduced to the value of a single bond ($P_{C^1C^3}$ = 1.102), the P_{CC} value of the C^1–C^2 bond has increased to 1.832 (Table 4). The calculated values for the ellipticity of the C–C bonds indicate that the π character of the C^1–C^2 bond in **3a** is nearly the same (ϵ_b = 0.397) as in **3** (ϵ_b =

Table 4. Calculated Results for the Allyl anions **3**–**3d** (For Details see Table 1)

	3	**3a**	**3b**	**3c**	**3d**
sym	C_2 (C_{2v})	C_s	C_s	C_s	C_s
E_{tot}	−116.79883(−116.39349)	−116.76185(−116.36094)	−116.75793(−116.35733)	(−116.38115)	(−116.34909)
E_{rel}	0.0 (0.0) *0.0*	22.8 (20.4) *23.1*	25.3 (22.7) *25.4*	(7.7) *7.4*	(27.9) *28.0*
i	0 (0)	1 (1)	1 (1)		
ZPE	37.4 (37.5)	36.9 (37.4)	37.0 (37.5)		
C^1–C^2	1.393 (1.382)	1.348 (1.331)	1.351 (1.334)	(1.331)	(1.382)
C^1–C^3	1.393 (1.382)	1.493 (1.508)	1.503 (1.518)	(1.508)	(1.382)
C^2–C^1–C^3	132.9 (133.7)	124.6 (125.9)	130.9 (131.3)	(133.1)	(127.3)
C^2–C^1–H^4–C^3	180.0 (180.0)	180.0 (180.0)	180.0 (180.0)	(180.0)	(180.0)
C^1–C^3–D	161.1 (180.0)	114.6 (113.9)	115.9 (115.5)	(180.0)	(119.0)
$P_{c^1c^2}$	1.652	1.832	1.831	1.760	1.801
$P_{c^1c^3}$	1.652	1.102	1.091	1.516	1.190

	3		**3a**		**3b**		**3c**		**3d**	
	$q(\rho(\mathbf{r}))$	q(NBO)	$q(\rho(\mathbf{r}))$	q(NBO)	$q(\rho(\mathbf{r}))$	q(NBO)	$q(\rho(\mathbf{r}))$	q(NBO)	$q(\rho(\mathbf{r}))$	q(NBO)
C^1	−0.040	−0.131	−0.029	−0.103	−0.003	−0.089	−0.052	−0.125	−0.074	−0.073
C^2	−0.328	−0.817	−0.228	−0.555	−0.246	−0.573	−0.268	−0.744	−0.250	−0.573
C^3	−0.328	−0.817	−0.380	−1.000	−0.402	−1.034	−0.402	−0.908	−0.316	−1.010
H^4	−0.067	0.154	−0.087	0.112	−0.066	0.138	−0.060	0.156	−0.111	0.087
H^5	−0.061	0.152	−0.050	0.150	−0.048	0.152	−0.050	0.153	−0.050	0.150
H^6	−0.057	0.153	0.000	0.182	−0.021	0.168	−0.058	0.154	−0.005	0.178
H^7	−0.057	0.153	−0.114	0.107	−0.106	0.119	−0.052	0.160	−0.099	0.121
H^8	−0.061	0.152	−0.114	0.107	−0.106	0.119	−0.055	0.154	−0.099	0.121
C^1H^4	−0.107	0.023	−0.116	0.009	−0.069	0.049	−0.112	0.031	−0.185	0.014
C^2H_2	−0.446	−0.512	−0.278	−0.223	−0.315	−0.253	−0.376	−0.437	−0.305	−0.245
C^3H_2	−0.446	−0.512	−0.608	−0.786	−0.614	−0.796	−0.509	−0.594	−0.514	−0.768

0.400). The covalent character of the C^1–C^2 bond, however, is clearly higher in **3a** ($H_b = -2.729$) than in **3** ($H_b = -2.177$, Table 2). The covalent character of the C^1–C^3 bond in **3a** ($H_b = -1.514$) is significantly lower than in **3** ($H_b = -2.177$).

The energy necessary to distort the C–C bond lengths in the planar form **3** to the values calculated for the transition state **3a** is 7.4 kcal/mol (Structure **3c**, Table 4). This is somewhat higher than the distortion energies calculated for the allyl cation and allyl radical. (See structures **1b** and **2b**, Tables 1 and 3.) Figure 3k shows the Laplacian distribution for the shortened C^1–C^2 bond of **3c** in the π plane of the bond. There is a visible charge accumulation at the terminal C^2 atom in the π direction. If the constraint of planarity is released in the geometry optimization of structure **3c**, while the C–C bond lengths are frozen, the C^2H_2 group adopts a strongly pyramidal geometry. The energy of the optimized form **3c** with a pyramidal C^2H_2 group is only 5.9 kcal/mol higher in energy than **3** [MP2/6-31G(d)//HF/6-31G(d)].

The optimized structure **3d** with a pyramidal C^3H_2 group and C–C bond length taken from **3** is 4.9 kcal/mol higher in energy than **3a** (Table 4). The calculated bond orders P_{CC} and charge distribution for **3c** and **3d** indicate that the electronic structure is not very different from **3** and **3a**, respectively. The planar form **3c** still has delocalized C–C bonds with bond orders $P_{C^1C^2} = 1.760$ and $P_{C^1C^3} = 1.516$, while **3d** has a C–C single bond ($P_{C^1C^3} = 1.190$) and a C–C double bond ($P_{C^1C^2} = 1.801$).

The theoretically predicted results for **3**–**3d** show that the allyl anion needs little energy for the distortion of the symmetric equilibrium structure **3** with identical C–C bond lengths toward **3c** with alternating C–C bond lengths, while the rotational barrier is quite high. Delocalization of π electronic charge is strong in both forms, **3** and **3c**.

6. Resonance Stabilization in Allyl Systms

The calculated data for the allyl cation, radical, and anion presented here give a coherent picture of the changes in the electronic structure upon rotation of a methylene group. Although the polarization of the C–C bonds and particularly the polarization of the π bonds varies among the three molecules, the qualitative features are the same. The nature of the C–C bonds in **1**, **2**, and **3** change from a delocalized π bond toward a C–C double bond and C–C single bond in the rotated forms **1a**, **2a**, and **3a**, respectively. What, then, is the reason for the significantly different rotational barriers in **1**, **2**, and **3**?

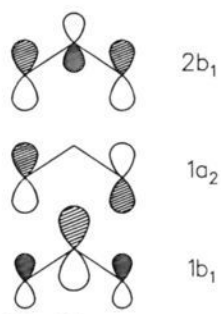

Figure 4. π orbitals of the allyl system.

Table 5. Calculated Barriers for Rotation of the CH_2 Groups ΔE (kcal/mol) at MP2/6-31G(d)//HF/6-31G(d), Charge Differences Δq at the CH_2 Groups between the Equilibrium Structures and Transition States.

	1	**2**	**3**
ΔE	37.8	12.6	23.1
Δq(NBO)	0.33	0.02	0.27
$\Delta q(\rho(\mathbf{r}))$	0.17	0.02	0.16

Figure 4 shows schematically the π molecular orbitals of the allyl system. The lowest lying $1b_1$ MO has a bonding character and is doubly occupied in **1**, **2**, and **3**. The next higher lying $1a_2$ MO is empty in **1**, singly occupied in **2**, and doubly occupied in **3**. Since the $1a_2$ MO is nonbonding, the rotation around the C–C bond is only hindered by the $1b_1$ π bond. It follows that the π bonding contributions in **1**, **2**, and **3** should induce similar rotational barriers for rotation of a methylene group.

Wiberg has advocated the role of electrostatic effects upon the rotational barrier of allyl ions.[6] Table 5 shows the calculated rotational barriers ΔE and the changes of the partial charges Δq at the rotated CH_2 groups for **1**–**3**. The allyl radical **2** has the lowest barrier (12.6 kcal/mol) and nearly no change in the charge distribution. The allyl anion **3** has a significantly higher barrier (23.1 kcal/mol). The change in the charge distribution at the rotated CH_2 group is 0.16 e using the topological analysis and 0.27 e using the NBO scheme. The highest rotational barrier

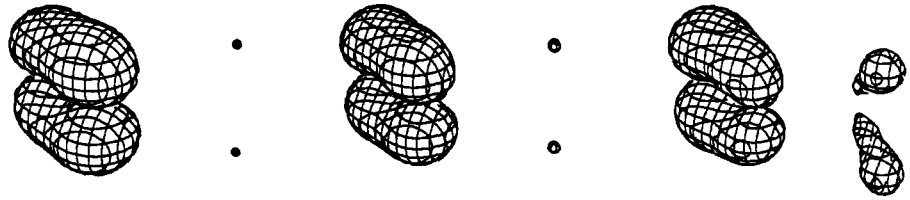

	1a			2a			3a		
	C^2	C^1	C^3	C^2	C^1	C^3	C^2	C^1	C^3
2a"	0.786	1.057	0.158	0.986	0.846	0.168	1.075	0.532	0.393
1a"	0.010	0.091	1.898	0.027	0.136	1.836	0.139	0.313	1.549

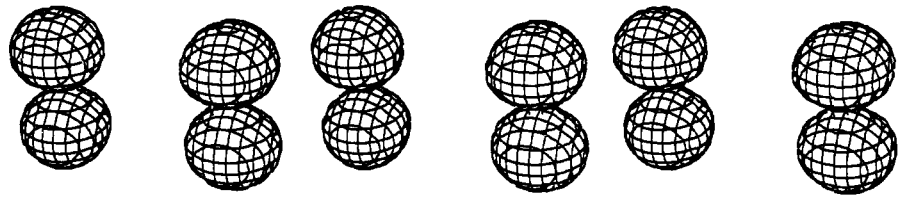

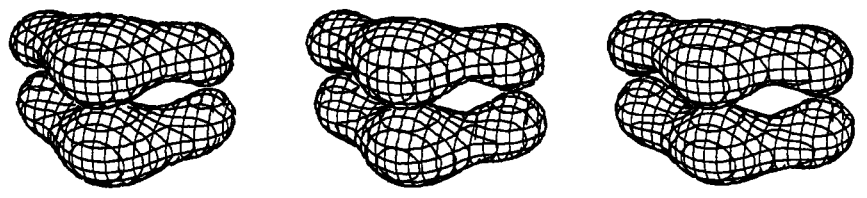

	1			2			3		
	C^2	C^1	C^3	C^2	C^1	C^3	C^2	C^1	C^3
$1a_2$	0.000	0.000	0.000	0.479	0.043	0.479	0.949	0.101	0.949
$1b_1$	0.503	0.993	0.503	0.530	0.942	0.530	0.576	0.849	0.576

Figure 5. Contour line diagrams of π orbitals of the planar equilibrium structures **1–3** (bottom) and the rotational transition states **1a–3a** (top) at HF/6-31G(d). Occupation of the p(π) orbitals at the carbon atoms calculated by integration of the electronic charge in the boundaries of the zero-flux surfaces. The occupation at C^3 in the 1a" and 2a" MOs include the hydrogen atoms of the C^3H_2 group.

(37.8 kcal/mol) and the largest change in the partial charge at the rotated CH_2 group (0.33 e using the NBO scheme, 0.17 e using the topological analysis) is calculated for the allyl cation **2**.

The calculated differences for the charge distribution should not be quantitatively overinterpreted. Any partitioning scheme for dividing the molecular charge distribution into atomic regions is based upon arbitrary assignments. Also the appealing proposal of using the mathematically well-defined zero-flux surfaces[10] to define atomic basins is only a model. In addition, the discussion in terms of point charges is not really appropriate for quantum mechanical properties. However, the data shown in Table 5 may be used for a plausible interpretation of the differences of the rotational barriers of **1**, **2**, and **3**. We suggest that the covalent contributions of the delocalized π bonding in **1**, **2**, and **3** to the rotational barriers have similar magnitude and that the significantly higher activation barriers of the cation **1** and the anion **3** are caused by the charge accumulation in the transition states. The planar forms **1** and **3** are stabilized relative to **1a** and **3a** not only by the π-bonding contribution, but also by the more favorable charge distribution associated with the π conjugation.

What is the reason for the allyl cation having a higher energy barrier for rotation of the CH_2 group than the anion? One reason may be the larger charge accumulation in **1a** and/or the different type of charge, i.e. positive charge in the cation rather than negative charge in the anion. We analyzed the electronic structure of the equilibrium forms **1**, **2**, and **3**, and the transition states for rotation **1a**, **2a**, and **3a** in more detail. Figure 5 shows the plots of the $1b_1$ and $1a_2$ π orbitals of **1–3** and the occupation at the carbon atoms, which are calculated by integration of the π-electronic charge in the boundaries of the zero-flux surfaces. The calculated electron population of the $1b_1$ MO for **1–3** is in good agreement with the Hückel approximation (1 electron at C^1, 0.5 electrons each at C^2 and C^3). Apart from a modest change in the polarization, the $1b_1$ MO in **1–3** changes very little. The occupation of the p(π) AO at the central carbon atom C^1 decreases slightly from **1** (0.993 e) to **2** (0.942 e) and **3** (0.849 e). As a consequence, the occupation of the p(π) AO at the terminal C atoms increases slightly from **1** (0.503 e) to **2** (0.530 e) and **3** (0.576 e). The $1a_2$ MO shows, for the radical and the anion, a small occupation at C^1, because the zero-flux surfaces do not coincide with the p(π) orbitals.

Figure 5 also shows the plots of the occupied π MOs of the transition states **1a–3a**, i.e. the 1a" and 2a" orbitals. The 1a"

MO is mainly located at the rotated CH_2 group and the 2a″ MO is mainly the C^1–C^2 π bond. The shape of the π orbitals and the calculated occupation at the carbon atoms shows clearly that the regions of the 1a″ and 2a″ MOs of **1a** and **2a** are well separated. However, the shape and the occupation of the π MOs of **3a** ar different! The 2a″ orbital extends over C^3 (occupation 0.39 electrons) and the 1a″ orbital has 0.45 electrons at C^1 and C^2. This means that the transition state **3a** is stabilized by hyperconjugation of the π electrons! The reason is, that the transition state **3a** has a *pyramidal* CH_2 group, while the CH_2 groups in **1a** and **2a** are planar. We calculated the allyl anion with a twisted *planar* CH_2 group. The optimized structure $CH_2CHCH_2^-$ with a perpendicular but *planar* CH_2 group is 32.9 kcal/mol higher in energy that the equilibrium structure **3** and 9.8 kcal/mol higher in energy than the transition state **3a** [MP2/6-31G(d)//HF/6-31G(d)]. This is comparable to the rotational barrier for the allyl cation (37.8 kcal/mol)! It follows that the lower activation barrier for rotation of a methylene group in the allyl anion than in the allyl cation is mainly due to the transition state **3a** being stabilized by hyperconjugation between the C–C π bond and the π orbital of the pyramidal CH_2 group. The pyramidalization of the CH_2 group lowers the rotational barrier significantly!

Now we examine the basis of Wiberg's reasoning that the allyl anion has small or negligible resonance stabilization.[6a,b] One reason is given as follows. Wiberg points out that the difference of the rotational barrier between the allyl cation (**1**) and anion (**3**) (estimated by him as 15 kcal/mol, calculated 14.7 kcal/mol in our study) is about what he estimates as the delocalization energy of **1** in the absence of strong charge interactions, using the delocalization energy of benzene as reference.[6a,b] Indeed, this is close to the calculated rotational barrier for the allyl radical (**2**) (12.6 kcal/mol). Structure **2** exhibits little charge alteration upon rotation. The author suggests that **1** is stabilized by delocalization (~15 kcal/mol) and additional electrostatic interaction (~23 kcal/mol). Since the latter value is the same as the total stabilization energy of the allyl anion (**3**), Wiberg concludes that the rotational barrier in **3** largely results from electrostatic terms.[6a,b]

Our results show that Wiberg's conclusion is not justified. The differences in the covalent π bonding in **1**, **2**, and **3** between the planar and rotated forms are very similar, as clearly demonstrated above. It is a coincidence that the difference of the rotational barriers of the allyl cation and the anion has the same magnitude as the rotational barrier of the allyl radical. Structure **1** has a larger barrier than **3** mainly because of the different charge interactions, and not because delocalization in **3** is not a stabilizing factor. Also, Wiberg does not recognize that the different charge interactions in the planar and rotated forms are only possible through delocalization of the π charge. This point is discussed below.

Another attempt to support the view that delocalization is not a stabilizing factor in **3** is based on the estimated change in electrostatic energy on rotation of the CH_2 group. Wiberg calculates the electrostatic energy of **3** and **3a** using the formula for the classical energy of a separated charge given by $7.2q^2/r$, where r is the radius in angstroms.[6b] He estimates that the size of the localized anion is about that of methane (~2 Å) and that of the planar anion is of the order of 3 Å. The difference in classical electrostatic energy would then be about 1 eV or 23 kcal/mol.[6b] This is close to the rotational barrier for **3**. We note that the estimated sizes of 2 and 3 Å for **3a** and **3** are totally arbitrary. Why should the size of **3a** be equal to that of methane? Also, the charge distribution is not uniformly spread over the molecules, which makes the use of a formula for the classical electrostatic energy of a isotropical charge distribution meaningless. The estimate of the change in electrostatic energy upon rotation in **3** cannot be considered as a serious scientific argument.

Wiberg argues that "one would expect the resonance stabilization of the allyl anion to be much less than for the cation as a result of the greater π electron repulsion in the anion."[6b] It will be shown in a forthcoming paper[19] that this statement is correct for the heavy-atom analogs $CH_2CHXH_2^{+/-}$ (X = Si, Ge, Sn, Pb). However, it is not correct for the parent allyl system! As discussed above, the resonance stabilization in the allyl systems is due to the delocalized nature of the $1b_1$ MO, which is shown in Figure 5. The shape of the orbital is nearly the same in the three compounds, which demonstrates that the stabilizing contribution of the conjugative interactions is comparable in magnitude.

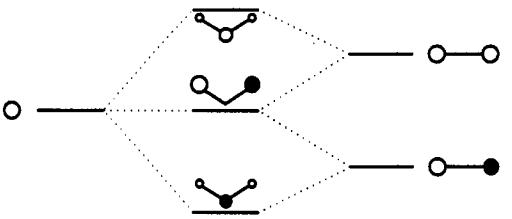

Figure 6. Interaction of a p(π) AO with a π and π^* MO.

Wiberg argues further that only in species in which electrons can be delocalized into π-deficient regions, can delocalization lead to π electron stabilization, and that no such regions are present in allyl anions.[6c] Figure 6 shows a diagram which indicates qualitatively the interactions between a π orbital and a p(π) AO. Stabilizing interactions in the allyl cation (**1**) arise from the interactions between the occupied π MO and the empty p(π) AO. The allyl radical (**2**) is stabilized by the conjugative interactions between the π and the π^* MOs with the singly occupied p(π) AO. In the allyl anion (**3**), the doubly occupied p(π) AO can also interact with both MOs, which yields the doubly occupied $1b_1$ and $1a_2$ orbitals showin in Figure 4. The π electronic charge is delocalized into the region between the carbon atom carrying the p(π) AO and the adjacent carbon atom, and a partial π bond is formed. It follows that π delocalization takes place in allyl anions as well as allyl cations and radicals.

Our objection to Wiberg's interpretation of resonance stabilization goes beyond the case of the allyl anion. The implicit assumption in his interpretations of the stability of numerous allylic systems[6] is that only the covalent contribution of the delocalization is considered as genuine resonance stabilization. The author makes a distinction between the energetic effect of delocalization due to covalent contributions, and the different electrostatic energies of the localized and delocalized charges. This difference, however, has nothing to do with the original concept of resonance energy! We may recall the definition of resonance energy, which is precisely given by Wheland in his fundamental study of resonance: "The *resonance energy*...is defined as the quantity obtained by subtracting the actual energy of the molecule from that of the most stable contributing structure."[20] No difference is made between the types of interactions which are associated with the delocalization of electronic charge in the conjugated system! We want to point out that the different charge distributions in the localized and delocalized forms, which cause different Coulomb interactions, are the result of the electron delocalization due to the conjugative interactions. It follows that, *conjugation is the origin of the greater stability of the planar forms of the allyl systems* **1–3**. The stabilization may become stronger by Coulomb interactions of accumulated charges associated with the delocalization.

We think that the statement made by Wiberg[6a,b] that the allyl anion has little resonance stabilization is not correct. The statement is based upon a misunderstanding of resonance energy as originally defined[20] and an inconsistent interpretation of the

(19) Gobbi, A.; Frenking, G. *J. Am. Chem. Soc.*, following paper in this issue.
(20) See ref 2, p 75.

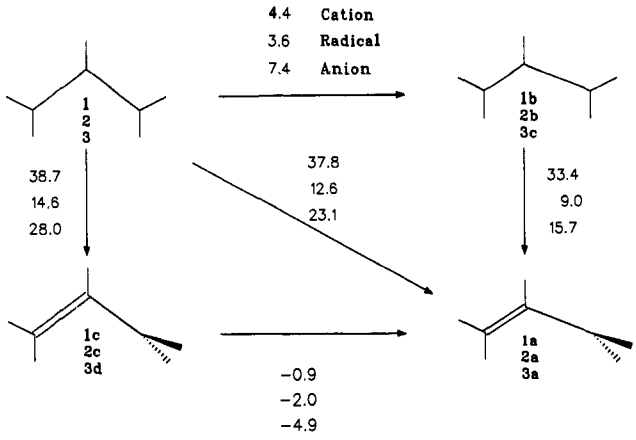

Figure 7. Calculated energy differences [MP2/6-31G(d)//HF/6-31G-(d)] for the allyl cation (top values), radical (middle values), and anion (bottom values). All values in kilocalories per mole.

electronic structure of the allyl anion. There is, in fact, significant resonance stabilization in the allyl anion!

7. σ and π Interactions in Allyl Systems

A second aspect of resonance and conjugation in π-delocalized systems, which has been debated for some time now, concerns the role of π conjugation upon the bond lengths in *planar* conjugated systems.[3-5] The center of the controversy is the question, whether π conjugation in systems like benzene or allyl radical favors symmetric structures with identical C–C bond lengths (D_{6h} for benzene, C_{2v} for allyl radical) or structures with alternate C–C bond distances (D_{3h} for benzene, C_s for allyl radical). The traditional view is that the resonance stabilization in these systems implies symmetric structures with identical C–C bond lengths. However, several theoretical studies led to the conclusion that π conjugation favors structures with alternate C–C bonds, and that the symmetric forms of benzene (D_{6h}) and the allyl radical (C_{2v}) are forced by the σ frame.[3,4] However, a very recent study by Glendening et al.[5] supported the traditional view, i.e. that "delocalization effects act to strongly stabilize symmetric benzene".

We think that there is a lot of confusion and misunderstanding in the literature about the role of π delocalization in conjugated systems. The results for the allylic system discussed above have shown that π delocalization is a strongly stabilizing factor, but that it is operative in the symmetric (C_{2v}) *and bond*-alternating (C_s) forms of the planar compounds. Delocalization strongly resists the rotation of the methylene groups, but not necessarily the C–C bond alternation. We want to demonstrate in the following that, while π delocalization is a strongly stabilizing factor in π conjugated systems, it does not necessarily lead to structures with identical C–C bond lengths. Figure 7 shows the energies which are associated with the distortions of the allyl systems **1**, **2**, and **3**.

The distortion of the equilibrium geometries of **1–3** in the corresponding transition state structures **1a–3a** can be broken up into the rotation of the CH_2 group (**1c**, **2c**, **3d**) and the change in the C–C bond lengths (**1b**, **2b**, **3c**). Figure 7 shows the calculated energies which are associated with the distortions. It becomes clear that the rotation of the methylene groups needs much more energy than the alteration of the C–C bond lengths of the planar structures from the C_{2v} forms to the C_s forms. There are two different effects operative in the rotation and bond alteration, although they are related to each other. The rotation of the methylene group switches the π conjugation off, while the alteration of the C–C bond lengths merely leads to *different* π interactions in the planar forms. Much confusion arises because the different processes which are involved with the rotation and bond alteration have been mixed up. For example, Shaik, Hiberty, et al.[3] (SH) theoretically analyzed the σ and π contribution of the change in the electronic energy for the process **2** → **2b**. They conclude that the symmetric C_{2v} form of the allyl radical **2** is favored over **2b** not because of π delocalization, but because the σ bonds enforce the symmetric structure. We will show below that we agree with this conclusion. However, we do not agree with SH, who say that "Electronic delocalization is, then, seldom expected to be a significant driving force in chemistry".[3b] Electron delocalization is a very strong driving force in chemistry, as demonstrated by the large rotational barrier for the allyl system. However, it is operative in both planar forms, the symmetric (C_{2v}) and bond alternated (C_s) structure. The different electronic interactions in these two forms of **1**, **2**, and **3** will now be analyzed in detail.

In order to estimate the different contributions of the σ and π electrons of the C–C bonds to the distortion, of the planar C_{2v} forms **1–3** to the C_2 structures **1b**, **2b**, and **3c**, we use the same method[21] as that suggested by SH for benzene and the allyl radical.[3b] The energy necessary for the distortion E_{dist} can be partitioned into the σ and π contribution of the electronic energy (E_σ and E_π) and the nuclear repulsion E_{NN}:

$$E_{dist} = E_\sigma + E_\pi + E_{NN} \quad (1)$$

The contribution of the nuclear repulsion is eliminated by calculating a distorted planar (C_s) form of the allyl system which has one long and one short C–C bond. The alteration of the C–C bond lengths is chosen such that the C_s form has the same nuclear repulsion energy as the C_{2v} form. The distorted C_s structures are shown in Table 6. The energy difference between these species and the corresponding equilibrium structures gives the change in the total electronic energy $E_{\sigma+\pi}$ arising from the C–C bond alteration. The calculated energies are also shown in Table 6.

$$E_{\sigma+\pi} = E_\sigma + E_\pi \quad (2)$$

In order to estimate the change of the σ part of the electronic energy E_σ, we calculated the same distortion of the allyl system in the absence of π delocalization. This was achieved in two different ways. For the first, we calculated the allyl trication which has empty p(π) orbitals at the carbon atoms. The other estimate of E_σ was made by calculating the quartet state of the allyl radical. Both methods may be criticized. The energy of the quartet state is influenced by exchange (Pauli) repulsion of the π electrons. The energy of the trication is influenced by the charge interaction. However, in the work by SH it could be shown that the distortion of the quartet state is influenced little by π interactions (<0.5 kcal/mol).[3b]

The calculated estimates of the σ contribution E_σ using the quartet state and trication as model systems are shown in Table 7. It is gratifying that both models give nearly the same results for the three systems, although the charge and the occupation of the p(π) orbitals are very different in the trication and the quartet. Therefore, it is reasonable to identify the calculated distortion energies as the energy contributions of the σ electrons alone. Also, the predicted σ contributions are nearly independent on the theoretical level, since the HF and MP2 results for E_σ are practically identical (Table 7).

The energy contributions E_π of the π electrons to the distortion from the C_{2v} form to the planar C_s form with a long and a short C–C bond may now be estimated as the difference between the

(21) Our method for estimating the different contributions of the σ and π electrons of the C–C bonds to the distortion energy is not exactly the same as used by SH.[3b] These authors keep only the nuclear repulsion between the carbon atoms constant, while in our method the distortion is chosen such that the *total* nuclear repulsion is constant. We have carried out the calculation using both methods and found that the results are nearly the same, the differences are ~0.1 kcal/mol.

Table 6. Calculated Results and Geometries for the Equilibrium Structures and Distorted Structures with Constant Nuclear Repulsion Energies (See Text)[a]

	radical		cation		anion	
	C_{2v}	C_s	C_{2v}	C_s	C_{2v}	C_s
E_{tot}^{MP2}	−116.80964	−116.80605	−116.54303	−116.53609	−116.78390	−116.77756
E_{tot}^{HF}	−116.46810	−116.46357	−116.19321	−116.18699	−116.39349	−116.38757
E_{rel}^{MP2}	0.0	2.3	0.0	4.4	0.0	4.0
E_{rel}^{HF}	0.0	2.8	0.0	3.9	0.0	3.7
C=C	1.391	1.331	1.373	1.313	1.382	1.322
C—C	1.391	1.454	1.373	1.436	1.382	1.446
C—C—C	124.5	124.5	118.1	118.2	133.7	133.6

[a] Calculated total energies, E_{tot} (hartrees); relative energies, E_{rel} (kcal/mol). Energies are given at the MP2/6-31G(d)//HF/6-31G(d) (MP2 and HF/6-31G(d)//HF/6-31G(d) (HF) levels of theory. Calculated bond lengths C–C (Å) and angles C–C–C (deg) are given at HF/6-31G(d)//HF/6-31G(d) level.

Table 7. Calculated Distortion Energies

	radical		cation		anion	
	MP2	HF	MP2	HF	MP2	HF
$E_{\sigma+\pi}$[a]	2.3	2.8	4.4	3.9	4.0	3.7
$E_{\sigma}^{trication_b}$	4.7	4.9	5.1	5.3	4.8	5.0
$E_{\sigma}^{quartet_b}$	4.8	4.9	5.2	5.3	4.9	5.0
$E_{\pi}^{trication_b}$	−2.4	−2.1	−0.7	−1.4	−0.8	−1.3
$E_{\pi}^{quartet_b}$	−2.5	−2.1	−0.8	−1.4	−0.9	−1.3

[a] For the distortion of the C_{2v} structures to the planar forms with one long and one short C–C bond (see Table VI). [b] σ- and π-contributions using the trication ($E_{\sigma}^{trication}$, $E_{\pi}^{trication}$) or using the ($^4A_1$) state ($E_{\sigma}^{quartet}$, $E_{\pi}^{quartet}$) as models.

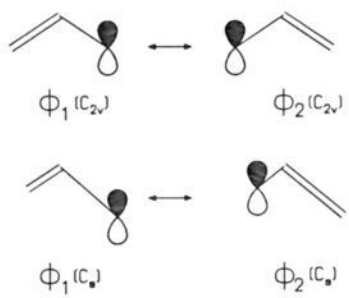

Figure 8. Resonance structures of the symmetric (top) and asymmetric (bottom) forms of the planar allyl system.

$E_{\sigma+\pi}$ and E_{σ} energies.[22] The calculations show (Table 7) that the E_{π} contributions have *negative* values. The results predict that the π part of the electronic energy favors the distorted structures by ~1–2 kcal/mol. It follows that the energy necessary for the distortion of the C_{2v} equilibrium forms of **1**, **2**, and **3** to a planar structure with one long and one short C–C bond is exclusively caused by the distortion of the σ frame of the C–C bonds. The present study demonstrates that the C_{2v} geometry of the allyl cation, radical and anion is enforced by the C–C σ bonds, and that the energy of the π electrons is slightly lower in the planar C_s forms. This has previously been shown for the allyl radical by SH.[3a,b]

The calculated results may be explained in terms of resonance structures. Figure 8 shows the resonance structures for the symmetric (C_{2v}) and distorted (C_s) forms of the allylic system. In the C_{2v} form both resonance structures have the same weight. In the C_s form the second resonance structure has less weight than the first structure (eqs 3 and 4). However, the second structure still contributes significantly to the energy. This becomes obvious by comparing the rotational barrier of the C_{2v} forms (38.7 kcal/mol for **1**, 14.6 kcal/mol for **2**, 28.0 kcal/mol for **3**) with the rotational barrier of the C_s forms of the allyl systems (33.4 kcal/mol for **1b**, 9.0 kcal/mol for **2b**, 15.7 kcal/mol for **3c**) shown in Figure 7.

$$\Psi(C_{2v}) = a\,\Phi_1(C_{2v}) + b\,\Phi_2(C_{2v}) \qquad a = b \tag{3}$$

$$\Psi(C_s) = a\,\Phi_1(C_s) + b\,\Phi_2(C_s) \qquad a > b \tag{4}$$

We want to comment on the recent publication by Glendening et al.[5] on the role of delocalization in benzene. These authors critisized the conclusion by SH[3] that the benzene σ framework is responsible for the symmetric structure, the π system preferring a distorted geometry. The authors noted that delocalization is strongly stabilizing not only in the symmetric (D_{6h}) form, but that "it is particularly noteworthy that delocalization strongly stabilizes *all* geometries, even highly distorted ones".[5] Yet, they came to the conclusion that "delocalization effects act to strongly stabilize symmetric benzene in essential accord with the concepts of classical resonance energy".[5] Although the investigated molecule is benzene and not the allyl system, we think that their conclusion and criticism of the work by SH[3] applies equally to the allyl system.

Glendening et al.[5] calculate the total delocalization energy in benzene using symmetric (D_{6h}) and distorted (D_{3h}) geometries. The calculations are based on the procedure introduced by Kollmar.[23] The authors use a partitioning scheme introduced by SH[3] for dividing the electronic part of the distortion energy into terms which are associated with the σ energy E_{σ} and π energy E_{π}. By using the same partitioning scheme to a localized wave function, they show that the distortion energy of the π electronic energy E_{π} has a sizable bond length dependence, even for a fully localized π system.[5] These authors say that "it appears therefore rather problematic to judge the role of delocalization based on the geometry dependence of E_{π}".[5] But SH have shown for the allyl radical that the same result, i.e. the dominant role of the σ frame imposing C_{2v} symmetry, is obtained when the geometry dependency of the E_{σ} part of the distortion energy is calculated using the procedure described above. Thus, at least for the allyl system it can be concluded that the C_{2v} geometry is enforced by the σ frame. It would be interesting to calculate benzene using the same method.

8. Summary

The equilibrium geometries of allyl cation (**1**) and allyl radical (**2**) calculated at HF/6-31G(d) have C_{2v} symmetry. A C_2 geometry with slightly pyramidal CH_2 groups is predicted at the MP2/6-31G(d) level for the allyl anion (**3**), but the energy difference to the planar C_{2v} form is negligible. The conjugation of the π electrons leads to strong resonance stabilization of the planar forms of **1**–**3**. The rotational barrier of a methylene group is significantly higher for the ions **1** and **3** than for the neutral

(22) It should be noted that in this method the energy contribution of the electron repulsion between the σ electrons and π electrons is taken as part of the π electron energy E_{π}.

(23) Kollmar, H. *J. Am. Chem. Soc.* **1979**, *101*, 4832.

radical **3**. This is explained by the accumulated charge in the transition states **1a** and **3a**. The necessary energy to rotate a methylene group in the allyl cation and allyl anion is similar in magnitude when the CH_2 group remains planar. Thus, resonance stabilization is higher in **1** and **3** than in **2**, because the delocalization in the allyl ions is associated with favorable charge distribution. The statement made by Wiberg[6] that the allyl anion has no resonance stabilization is repudiated. The analysis of the electronic structure shows that the conjugative contribution to the resonance stabilization is comparable in magnitude in **1–3**. Also, resonance stabilization, as originally defined, includes conjugative stabilization as well as the Coulomb interactions associated with the delocalization.

The calculations for structures with alternating C–C bond lengths show that planar distorted forms are also strongly stabilized by π conjugative interactions. The calculated σ electronic part of the distortion energies, using a quartet state or a trication as model system, indicates that the π electronic energy favors a planar form with one short and one long C–C bond for **1–3**. It is the σ electronic energy which enforces equal C–C bond lengths in the allyl systems.

Acknowledgment. This work has been supported by the Deutsche Forschungsgemeinschaft and the Fonds der Chemischen Industrie. We acknowledge generous support and excellent service by the computer centers HRZ Marburg, HHLRZ Darmstadt, HRZ Giessen, HRZ Frankfurt, and HLRZ Jülich.